arXiv:cond-mat/0408413v1 [cond-mat.supr-con] 18 Aug 2004

Anomalous Peaks in the Fourier Transformed Density of States of a Bilayer D-Wave Superconductor

K. M. Stevens and W. A. Atkinson
Trent University
(Dated: May 23, 2019)

The Fourier transformed density of states (FTDOS) has been shown to be a useful tool for analyzing the electronic excitation spectrum of high temperature superconductors. The most widely studied material, $Bi_2Sr_2CaCu_2O_8$, is a bilayer material, with two two-dimensional CuO_2 layers per unit cell. We explore the effect of coupling between CuO_2 layers on the FTDOS. We find that peaks in the spectrum are split by the bilayer coupling by an amount which is proportional to the coupling constant $t_\perp$. In addition, we find a new set of anomalous dispersing peaks which arise from a crossing of bonding and antibonding bands, and which occur only in the superconducting state. These peaks are typically much stronger than any peaks found in the one-layer spectrum, are pointlike rather than cusplike, and lie close to the single-layer peak positions. Experimentally, the anomalous peaks can be distinguished from the conventional peaks by their persistence to energies above the coherence energy.

I. INTRODUCTION

Many of the most commonly studied high temperature superconductors (HTS) are bilayer materials, containing two parallel two-dimensional CuO_2 planes in each unit cell. Early density function theory calculations predicted that the quasi-two-dimensional bands associated with mobile holes in the CuO_2 layers should hybridize to form bonding and antibonding bands in the bilayer materials.[1,2] Until recently, angle resolved photoemission spectroscopy (ARPES) experiments in $Bi_2Sr_2CaCu_2O_8$ (BSCCO) have failed to see the predicted splitting,[3] apparently indicating that strong correlations inhibit coherent electron hopping between layers.[4] In the past few years, however, improvements in experimental techniques have permitted ARPES experiments to resolve a pair of bands dispersing across the Fermi energy.[5,6,7,8,9,10] While the bands are most easily resolved in overdoped materials, the magnitude of the bilayer splitting seems to be more or less independent of doping, and to persist to underdoped materials.

A complementary technique, scanning tunneling microscopy (STM), has also provided valuable insight into the electronic structure of HTS. It was shown[11] that spatial maps of the local density of states (LDOS) $(\mathbf{r};!)$ at constant energy $!$ can be used as a probe of the quasiparticle excitation spectrum. The essential idea is that impurity scattering produces standing wave patterns (Friedel oscillations) in $(\mathbf{r};!)$. The q-vectors in the Fourier transform $(\mathbf{q};!)$ directly give the difference $\mathbf{q} = \mathbf{k}_{scatt.} - \mathbf{k}_{inc.}$ between scattered and incident quasiparticle wavevectors. If $(\mathbf{q};!)$ is peaked at a certain wavevector $\mathbf{q}$, it indicates either that the impurities preferentially scatter through $\mathbf{q}$, or that there is a large density of initial and final scattering states connected by $\mathbf{q}$. The latter effect depends only on the quasiparticle dispersion, and for a random collection of structureless impurities should be the dominant effect. The technique of Fourier transforming the LDOS is commonly known as Fourier transform spectroscopy.

Fourier transform spectroscopy has been widely used to study the superconducting[12,13,14,15] and normal state[16] spectra of HTS. In the superconducting state, a particularly simple analysis[17,18,19,20,21,22] appears to satisfactorily explain the basic qualitative features of the dispersing peaks in the Fourier transformed density of states (FTDOS), although the quantitative aspects of the FTDOS in HTS have always been problematic. The general conclusion of this work is that, in most aspects, the STM experiments of Refs. [12,13] on overdoped BSCCO appear to be consistent with the simple picture of dispersing, BCS-like quasiparticles in a d-wave superconductor.

Since ARPES experiments have succeeded in measuring the splitting of the Fermi surface in BSCCO due to bilayer coupling, it is natural to ask whether the same splitting can be seen in STM experiments. In this work we show that, in accordance with naïve expectations, peaks in $(\mathbf{q};!)$ are split by bilayer coupling. Unless the coupling is large, however, it may be difficult to observe because of the noise introduced by randomness in the impurity positions.[18,20] We also show that there are novel anomalous peaks arising from a combination of interlayer tunneling and superconducting pairing. The terminology anomalous reflects the fact that the peaks result entirely from the anomalous (off-diagonal) quasiparticle propagator. These peaks are extremely strong compared with other peaks and should be easily visible in experiments.

We describe the calculations in section II, and show that the FTDOS is related to a response kernel $_{ij;}(\mathbf{q};!)$ which depends only on the dispersion of the clean BSCCO bands. The results are discussed in section III and conclusions appear in section IV.

II. CALCULATIONS

We consider a simple model of two identical superconducting layers coupled via coherent quasiparticle hopping. We assume that the STM experiment measures only the LDOS $_1(\mathbf{r};!)$ in the top layer (layer 1). The

Hamiltonian is

$$H = \sum_{k,\ j=1}^{} \Big[\sum_{}^{2} {}_k c^{y}_{jk\ } c_{jk\ } + t_\perp(k)\ c^{y}_{1k\ } c_{2k\ } + h.c. \Big] + \sum_{k\ \ j=1}^{\ \ \ \ 2} {}_k\ c^{y}_{jk"} c^{y}_{j\ \ k\#} + h.c.; \quad (1)$$

where c^{y}_{jk} is a creation operator for an electron in layer j with wavevector k and spin $\ $, $t_\perp(k) = \frac{t_\perp}{4}[\cos k_x - \cos k_y]^2$ is the interlayer tunneling matrix element,[4,23] and ${}_k = \frac{{}_0}{2}[\cos(k_x) - \cos(k_y)]$ is the d-wave superconducting order parameter. A reasonably realistic model of the quasiparticle dispersion in overdoped BSCCO is given by taking ${}_k = t_0 + 2t_1(\cos(k_x) + \cos(k_y)) + 4t_2\cos(k_x)\cos(k_y) + 2t_3[\cos(2k_x) + \cos(2k_y)]$ with $\{t_0;\ldots;t_3\} = \{430;\ 400;90;\ 82\}$ meV.[24] In the normal state, the band energies are ${}_{(A;B)k} = {}_k \mp t_\perp(k)$ where A (B) corresponds to the upper(lower) sign. The maximum splitting, which occurs at $(\ ;0)$ and $(0;\ )$, is $\max({}_{Ak} - {}_{Bk}) = 2t_\perp$. Values of $t_\perp$ extracted from experiments[5,7,24] range from 45 meV to 82 meV, and appear to be independent of doping.[10,24,25] In this work we take $t_\perp = 82$ meV and ${}_0 = 60$ meV. In the superconducting state, the Hamiltonian has two positive and two negative energy bands

$$E_{(A;B)k} = \sqrt{{}^{2}_{(A;B)k} + {}^{2}_{k}}.$$

In the following discussion, we will describe how to extract information about the bands of the pure superconductors from the FTDOS of the disordered superconductor. In the end, we will argue that the details of the impurity potential are of secondary importance, and that the q-space structure of ${}_1(q;!)$ is given by a linear combination of response kernels ${}_{ij;\ }(q;!)$ which depend only on the band structure of the pure material. Since there are already a number of comprehensive discussions of the response kernel (see especially Ref. [20]), the current discussion will be cursory, and will only highlight differences arising from the bilayer band structure. For those who are not interested in the details of the calculation, and who choose to skip to the next section, we remark that the subscripts i and j refer respectively to the layer in which the FTDOS is measured and the layer in which the impurity scattering takes place. The subscript $\ \ 2\ f0;\ldots;3g$ denotes the different channels in Nambu particle-hole space, and indicates different ways in which impurity scattering may mix hole and electron states. For purposes of this work, the different channels behave sufficiently similarly that we will only consider $\ = 3$.

We assume that each layer has independently-distributed random disorder. For simplicity, we adopt a model of pointlike impurities with potential $V(r) = V\ _{r;0}$ (for an impurity at the origin). The single-impurity scattering T-matrix describes scattering from $V(r)$ to all orders of perturbation theory, and is $\hat{T} = [\hat{}_0 \quad V\ \hat{}_3\hat{g}(!)]^{\ 1}$ where $\hat{g}(!) = N^{\ 1}\sum_k \hat{G}(k;!)$, N is the number of points in k-space, and $\hat{G}(k;!)$ is the $2\ \ 2$ Green's function matrix in Nambu space.[18] Here, the $\hat{}$ indicates a matrix in Nambu particle-hole space and $\hat{}_0$ and $\hat{}_3$ are Pauli matrices. The T-matrix can be decomposed into Nambu components: $\hat{T} = T_0\hat{}_0 e^{i\ 0} + T_3\hat{}_3 e^{i\ 3}$, where T and $\ $ are the $!$-dependent scattering amplitudes and phase-shifts respectively. For pure potential scattering, $T_1 = T_2 = 0$.

For a sufficiently dilute concentration of randomly distributed impurities, we can break the FTDOS in layer 1 into two contributions: ${}_1(q;!) = {}_{11}(q;!) + {}_{12}(q;!)$ where ${}_{1j}(q;!)$ describes contributions from scattering events in layer j. We can show that for a collection of N_{imp} identical scatterers in each layer,[18]

$$ {}_{1j}(q;!) = \frac{1}{\ } \sum_{\ =0}^{3} T_j\ (q;!)\,\mathrm{Im}\,[e^{i\ (!)}\ {}_{1j;\ }(q;!)] \quad (2)$$

where $T_j\ (q;!) = \sum_{i=1}^{N_{imp}} T\ e^{\ iq\ R_i^{(j)}}$ and $R_i^{(j)}$ is the position of the i^{th} impurity in layer j. The response kernels were first defined for a single layer in Ref. [20], and are easily generalized to the bilayer situation here: ${}_{1j;\ } = N^{\ 1}\sum_k [L_{1j}(q;!) \mp M_{1j}(q;!)]$ where the upper (lower) sign corresponds to $\ = 0$ ($\ = 3$), where

$$L_{1j}(q;!) = \frac{1}{N}\sum_k G_{1j}(k;!)G_{j1}(k+q;!); \quad (3)$$

$$M_{1j}(q;!) = \frac{1}{N}\sum_k F_{1j}(k;!)F_{j1}(k+q;!); \quad (4)$$

and where $G_{ij}(k;!)$ and $F_{ij}(k;!)$ are electron and anomalous Green's functions. The subscripts refer to the layer index, ie. $G_{12}(k;!)$ refers to an electron whose path originates in layer 2 and terminates in layer 1. We refer to $L_{1j}(q;!)$ and $M_{1j}(q;!)$ as the electron and anomalous response kernels respectively. From Eq. (1), the various Green's functions are

$$G_{11}(k;!) = \frac{(\dot{!} + {}_k)(\dot{!}^2 \quad {}^{2}_{k} \quad {}^{2}_{k}) \quad t_\perp(k)^2(\dot{!} \quad {}_k)}{D};$$

$$G_{12}(k;!) = \frac{t_\perp(k)[(\dot{!} + {}_k)^2 \quad t_\perp(k)^2 + {}^{2}_{k}]}{D};$$

$$F_{11}(k;!) = \frac{{}_k(\dot{!}^2 \quad {}^{2}_{k} \quad {}^{2}_{k} + t_\perp(k)^2)}{D};$$

$$F_{12}(k;!) = \frac{2\ {}_k\ {}_k t_\perp(k)}{D};$$

with $D = (\dot{!}^2 \quad E^2_{Ak})(\dot{!}^2 \quad E^2_{Bk})$. Throughout this work, $\dot{!} = ! + i$ where $!$ and $\ $ are real and $\ $ is small and positive (we take $\ = 2$ meV for numerical calculations).

Equation (2) shows that the FTDOS is a linear combination of several response kernels, and that the effect of randomness in the impurity positions is to modulate the response kernels by a random prefactor $T_j\ (q;!)$. Since the prefactor is featureless, the q-space structure of ${}_1(q;!)$ is determined by ${}_{1j;\ }(q;!)$. The noise introduced by the prefactor can be a significant issue, and has

been discussed extensively elsewhere[18,20] with the main conclusion being that, at this level, disorder tends to obscure (rather than broaden, as one might naively expect) structure in the FTDOS. Weak extended scattering potentials have also been studied, and similar conclusions have been reached, although the FTDOS is further modulated by the form factor of the impurity potential.[20] For extended impurities which are not significantly larger than the Fermi wavelength, the impurity form factor does not significantly modify the peak structure of the FTDOS. It appears, then, that for most kinds of randomly distributed dilute disorder, the structure of $_1(q;!)$ is essentially that of the response kernels.

III. DISCUSSION

As shown in Eq. (2), the FTDOS in the top layer is a linear combination of several response kernels, modulated by a random prefactor. An explicit calculation of $_1(q;!)$ requires a detailed knowledge of the impurity potential. However, since we are only interested in identifying qualitative trends, and since all of the response kernels behave in a similar fashion, we can safely limit our discussion to a single component, $_{11;3}(q;!)$. This simplifies the discussion considerably, but does not change any qualitative conclusions. In particular, it has no effect on the novel anomalous peaks reported below.

A second comment regarding Eq. (2) is that, because of the phase of the T-matrix, both real and imaginary components of $_{1j;}(q;!)$ contribute to $_1(q;!)$. Most theoretical work to date has focussed on the imaginary part of the kernel since most calculations are in the weak scattering limit where $\to 0$. In the absence of a detailed model of the scattering phase shifts, we find it simplest to study the magnitude of the complex response kernel. Again, this does not affect our conclusions.

Figure 1 provides a comparative illustration of the evolution of the response kernel as a function of energy. When $|!| \ll _0$, there is little difference between single layer and bilayer superconductors [Fig. 1(a) and (e)]. As $|!|$ increases, however, two differences appear [Fig. 1(b) and (f)]. First, a new set of peaks appears in the bilayer spectrum which is not present in the single layer spectrum. Second, features present in the single layer spectrum are broadened or split in the bilayer spectrum. The new peaks, termed anomalous because they originate from the anomalous (superconducting) piece of the Green's function, persist to energies $\sqrt{^2_0 + t_?^2}$ [Fig. 1(c) and (g)], beyond which they vanish abruptly [Fig. 1(d) and (h)]. There is, therefore, a window of energies which are larger than the coherence peak energy ($_0$) where the single layer peaks have disappeared but the bilayer peaks persist [Fig. 1(c) and (g)]. The bilayer splitting is most clearly resolved when $|!| > \sqrt{^2_0 + t_?^2}$ [Fig. 1(d) and (h)]. These are the main results of this paper, and the remainder of this section is devoted to understanding them.

To begin with, we briefly discuss the single layer system. When $|!| < _0$, the kinds of plots shown in Fig. 1 are typically interpreted in terms of a "banana" model (see eg. Ref. [13]), in which quasiparticles are scattered through a wavevector q between different points on the constant energy contours with energy $!$. Peaks in $|_{11;3}(q;!)|$ are supposed to correspond to transitions with a high joint density of states. In the superconducting state, for a single layer d-wave superconductor, the energy contours have a characteristic "banana"-shape, shown in Fig. 2(a), and the joint density of states is largest for transitions connecting the tips of the "bananas". Although it has been argued that this interpretation is too simplistic,[21] it appears to work qualitatively for the single layer superconductor. Two predicted transitions, labelled q_5 and q_7, are shown in Fig. 1(b). Both correspond to actual peaks in the response kernels, although the q_5 peak is quite weak because of selection rules [it appears more strongly in $_{11;0}(q;!)$]. We remark that although experiments appear to see peaks in locations predicted by the "banana"-analysis, calculations of the response function actually find a good deal more structure than is seen experimentally. In part, this may be because the disorder-related noise hides the structure in experiments,[18] but it may also be an indication that the current picture of tunneling in BSCCO is incomplete. One suggestion, for example, is that nanoscale inhomogeneities in the quasiparticle spectrum have a quantitative effect on the shape of the peaks in the FTDOS.[26]

Figure 2(b) shows that the effect of interlayer coupling is to split the constant energy contours into a pair of bonding and antibonding "bananas". Because of the form of $t_?(k)$, the degree of splitting depends strongly on k. The "bananas" are centered at the nodal points where $t_?(k) = 0$, and the splitting is greatest at the tips of the "bananas" where $t_?(k)$ is largest. Since the size of the "bananas" is roughly proportional to $|!| = _0$, where $|!| = _0 = 1$ is the approximate energy at which the tips of the "bananas" reach the Brillouin zone boundary, it follows that the splitting is also approximately proportional to $|!| = _0$.

Since the splitting of bonding and antibonding bands is small for $|!| = _0 \ll 1$, it is unsurprising that the plots of the single layer and bilayer response kernels in Fig. 1(a) and (e) are very similar. As $|!| = _0$ increases, we begin to see the effects of bilayer coupling. Since the interlayer hopping doubles the number of bands, we expect to see a splitting of each peak into a quartet of closely-spaced peaks corresponding to transitions within and between the bonding and antibonding bands. The peak spacing is expected to be proportional to $t_?$ and to grow with $|!|$. Note that, because of the strong k-dependence of $t_?(k)$, not all peaks are equally split, and that the largest splitting occurs for features coming from transitions between states near the Brillouin zone boundary [such as the q_1 peak in Fig. 2(a)]. At most energies, the splitting cannot be resolved, and appears as a broadening of the response kernel, with a corresponding reduction in peak heights

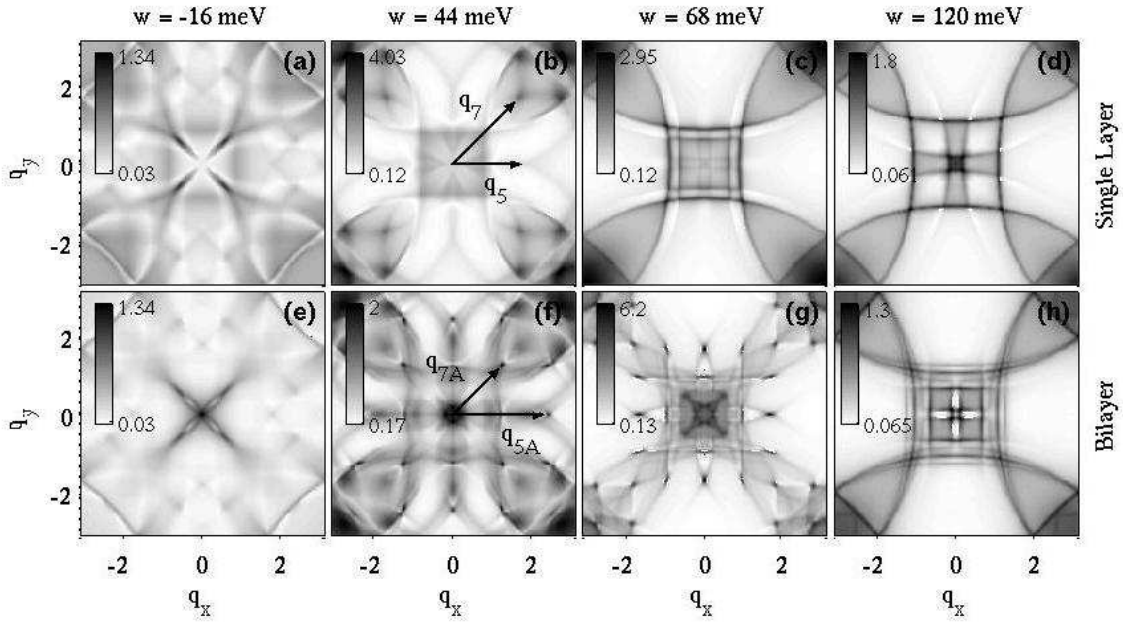

FIG. 1: Response kernel for single layer and bilayer superconductors. $j_{11;3}(q;!)j$ is shown for (a)–(d) a single layer and (e)–(h) a bilayer superconductor, for (a),(e) $! = 16$ meV, (b),(f) $! = 44$ meV, (c),(g) $! = 68$ meV and (d),(h) $! = 120$ meV. These plots are characteristic of the four regimes $j!j \ll {}_0$, $j!j$ less than, but of order ${}_0$, ${}_0 < j!j < \sqrt{{}_0^2 + t_?^2}$ and $j!j > \sqrt{{}_0^2 + t_?^2}$. Arrows in (b) and (f) indicate the positions of several peaks expected from simple analyses of the band structure, illustrated in Fig. 2. Images are 200×200 pixels and have been smoothed over 5 pixel windows for presentation.

[compare, eg. Fig. 1(b) and (f)]. The band splitting appears most clearly in the normal state, and at energies $j!j > \sqrt{{}_0^2 + t_?^2} \approx 100$ meV (the significance of this energy is discussed below), where the anomalous peaks vanish. In general, bilayer splitting might be difficult to resolve in an experiment because of disorder-related noise, and might simply broaden spectral features.

As we have already said, peak splitting is not the dominant effect of bilayer coupling unless $j!j > \sqrt{{}_0^2 + t_?^2}$. Rather, it is the new anomalous peaks which dominate the spectrum when $j!j \ll {}_0$. These peaks are narrow and can be orders of magnitude larger than the "banana"-tip peaks. The peak positions are not at the positions predicted by the "banana"-analysis, though they disperse in a qualitatively similar fashion. Most notably, these peaks grow rapidly in intensity as $!$ increases, to the point where they are the dominant feature in the spectrum by 68 meV.

The anomalous peaks arise from the points at which the bonding and antibonding bands cross [Fig. 2(b)]. For this reason, the anomalous peaks are much more point-like than the convential single layer "cusplike" peaks. If we denote one of the crossing points by $k_0 = (k_{0x}; k_{0y})$, then the remaining crossing points are connected to it by vectors $q_{1A}; :::; q_{7A}$, as shown in Fig. 2(b). The q_{5A} and q_{7A} arrows in Fig. 1(f) are determined from the energy dispersions, and confirm that the anomalous peak positions are given by transitions between the crossing points. The points k_0 satisfy $j!j = E_{A k_0} = E_{B k_0}$, corresponding to the simultaneous conditions $_{k_0} = 0$ and $!^2 = {}_{k_0}^2 + t_?^2 (k_0)^2$. The energies $! = \sqrt{{}_0^2 + t_?^2}$ are the approximate energies at which the crossing points leave the Brillouin zone, and are therefore also the energies at which the anomalous peaks must vanish.

In Fig. 1, it is clear that, except at small $j!j$, the anomalous peaks are much stronger than the corresponding single-band peaks. The strongly divergent behavior comes from the fact that the anomalous Green's function $F_{11}(k;!)$ has a second order pole at the crossing point: ie. $F_{11}(k_0;!) = 2t_?^2 (k_0)^2 {}_{k_0}/(2!)^2$. In contrast, $G_{11}(k;!)$, $G_{12}(k;!)$, and $F_{12}(k;!)$, have cancellations which reduce the order of the pole so that, for example, $G_{11}(k_0;!) = (2i)^{-1}$. After summing over k in Eq. (3), the product of first order poles in $G_{11}(k;!)$ and $G_{11}(k+q;!)$ becomes a single first order pole in $L_{11}(q;!)$. The singularity is more severe in Eq. (4); the product of second order poles, when summed over k, yields a second order pole. To illustrate this, we evaluate the contribution of the poles to $M_{11}(q_{5A};!)$ analytically. Taking k near k_0, and letting q_{5A} be the wavevector

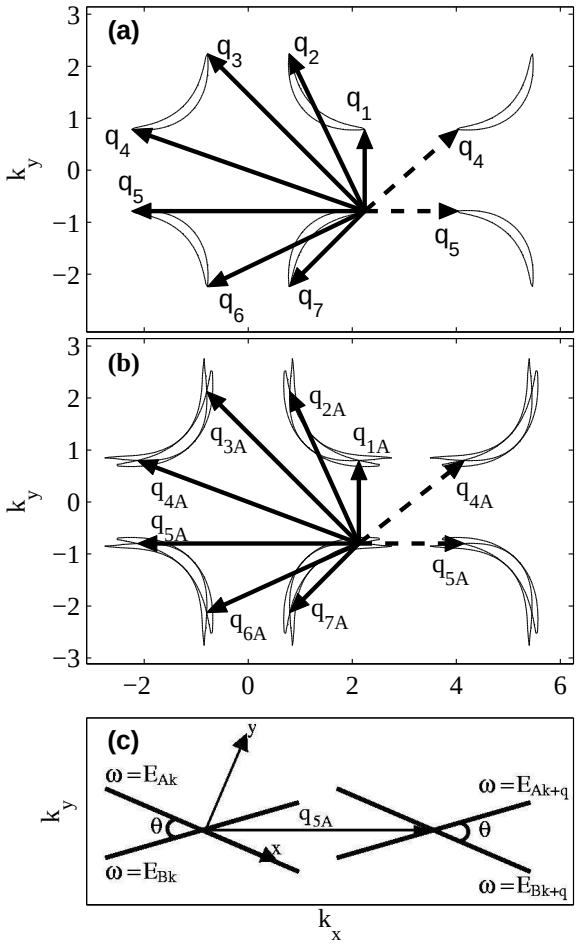

FIG. 2: Scattering transitions in d-wave superconductors. Contours at a fixed energy are sketched for (a) single layer and (b) bilayer superconductors. In single layer systems, the joint density of states is largest for transitions, indicated with arrows labelled q_1,...,q_7, connecting tips of the energy contour "bananas". In bilayer systems, the dominant transitions, labelled q_{1A},...,q_{7A}, connect crossing points of the bonding and antibonding bands. Dashed arrows show the mapping of q-vectors into the first Brillouin zone. A sketch of the q_{5A} transition is shown in (c), with definitions of the variables used in deriving Eq. (5).

shown in Fig. 2(b), we can write

$$F_{11}(k;\omega) \quad \frac{t_\perp^2 (k_0)^2 \quad {}_{k_0}}{2\omega^2 (\omega \quad E_{Ak})(\omega \quad E_{Bk})}$$

$$F_{11}(k + q_{5A};\omega) \quad \frac{t_\perp^2 (k_0)^2 \quad {}_{k_0}}{2\omega^2 (\omega \quad E_{Ak+q_{5A}})(\omega \quad E_{Bk+q_{5A}})}$$

Defining orthogonal axes x and y as shown in Fig. 2(c), we have

$$\begin{aligned}
\omega \quad E_{Bk+q_{5A}} &= y + i \\
\omega \quad E_{Ak+q_{5A}} &= x\sin \quad y\cos \quad + i \\
\omega \quad E_{Bk} &= y\cos \quad x\sin \quad + i \\
\omega \quad E_{Ak} &= \quad y + i :
\end{aligned}$$

We have made the approximation that the two constant energy contour crosses illustrated in Fig. 2(c) are aligned with one another. This approximation is fairly good at larger values of ω, where the anomalous peaks are most pronounced. Then, the intensity of the q_{5A} peak is

$$M_{11}(q_{5A};\omega) \quad \int \frac{dxdy\, C\,(k_0)^2}{(y^2 + \quad ^2)[(x\sin \quad y\cos \quad)^2 + \quad ^2]}$$
$$= \frac{C\,(k_0)^2 \quad ^2}{^2 \sin \quad}; \qquad (5)$$

where $C(k_0) = t_\perp^2 (k_0)^2 \quad {}_{k_0}/2[t_\perp^2 (k_0)^2 + \quad {}^2_{k_0}]$. The factor $C(k_0)$ is a strong function of k_0, and consequently of energy since the crossing point location is determined by ω, vanishing at the nodal point and rising as $(\cos k_{x0} \quad \cos k_{y0})^3 \quad \omega^3$ at low ω. Thus, the intensity of the anomalous peaks grows as ω^6 at small ω.

Similar calculations have been performed for $M_{11}(q;\omega)$ for each of the q-vectors shown in Fig. 2(b), and all have a second order pole (ie. all are proportional to $\quad ^2$) with the exception of q_{1A} and $q = 0$, which vanish. If the crossing point axes illustrated in Fig. 2(c) are not aligned, then q_{1A} will not vanish identically, but should still be weaker than other peaks. These results are in accord with our numerical calculations. Furthermore, as suggested above, $M_{11}(q;\omega)$ is the only one of the four response functions defined in Eqs. (3) and (4), to have a second order divergence.

Figure 3 shows both the intensity and dispersion of the response kernel. For the single layer system, q_1 and q_5 can be seen dispersing up to $\omega \quad _0$, at which point the "banana"-tips pass through the Brillouin zone boundary, and the dispersion begins to look more like the normal state dispersion. For the bilayer system one can see, in addition to the q_5 feature, the strong q_{5A} peak and a weaker q_{1A} feature. As expected from Eq. (5), the intensity of the q_{5A} peak is a strong function of energy and by 50 meV is the dominant feature in the spectrum (note that the color scale is logarithmic). The q_{5A} peak disperses up to $\omega \quad \sqrt{{}^2_0 + t_\perp^2}$, at which point the crossing points pass through the Brillouin zone boundary. Above this energy, the spectrum begins to look like that of the bilayer system in the normal state, and it is here that one can resolve the splitting of the transitions by the interlayer coupling most clearly. The dispersions of the anomalous peaks are shown in Fig. 3(c). Except at higher energies, the anomalous peak positions are very near to the conventional peaks of the single layer systems, and might be difficult to distinguish in an experiment.

We finish this section by speculating that the peaks seen in some existing Fourier Transform spectroscopy

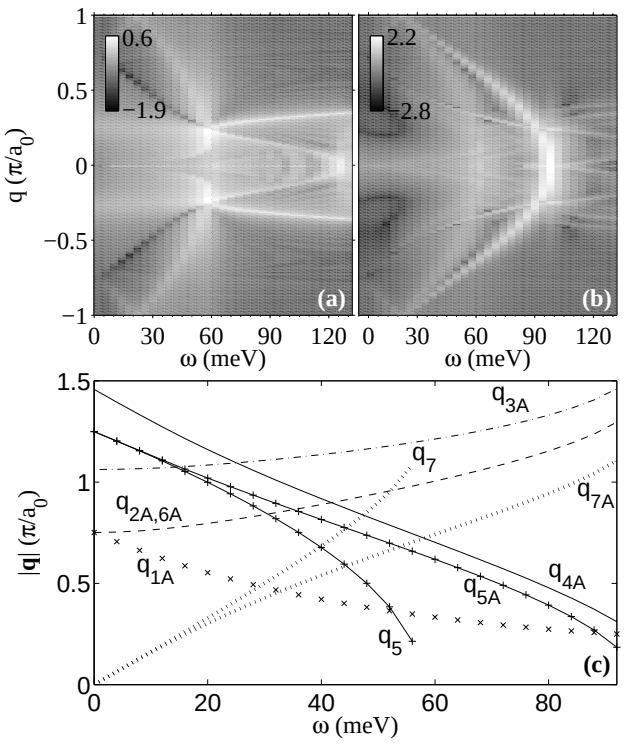

FIG. 3: Dispersion of $j_{11;3}(q;!)j$. Intensity plot of $\log j_{11;3}(q;!)j$ for (a) the single layer and (b) bilayer systems, where $q = (q;0)$. meV. Dispersions of the anomalous peaks are shown in (c). Also shown for comparison are dispersions for the single layer peaks q_5 and q_7.

experiments might actually be the bilayer peaks discussed here. The question is this: if one calculates $_1(q;!)$ for a bilayer, and then interprets the spectrum in terms of a single-band "banana" model, what does one find? Interestingly, since the crossing points actually lie on the Fermi surface for the isolated layer, one would extract the correct Fermi surface. However, because the crossing points disperse more slowly than the "banana"-tips, one would overestimate the gap: $^{\text{apparent}}_{k} = \sqrt{(k)^2 + t_?(k)^2}$. Experimentally, McElroy et al[13] found that the angle-dependent gap was larger than the gap measured in ARPES experiments, consistent with our expectations. On the other hand, the predicted anomalous peak amplitudes are strong functions of $!$, in contrast with these same experiments. It is possible that, to a large extent, this could be mitigated by inelastic scattering effects. The anomalous peak height is proportional to ^{2}. If grows with $!$, as is widely suggested, then this may offset the predicted peak height growth. Perhaps the most important distinction between the anomalous and single-layer peaks is that the former disperse more slowly, and continue to be present at energies $_0 < ! < \sqrt{^2_0 + t^2_?}$ where the single layer peaks have disappeared.

IV. CONCLUSIONS

Coherent coupling between the layers of bilayer $Bi_2Sr_2CaCu_2O_8$ has now been observed in ARPES experiments at doping levels ranging from overdoped to weakly underdoped. We have shown that bilayer coupling should also be apparent in Fourier transform spectroscopy experiments at similar doping levels. Bilayer coupling is manifested in two ways: first through a splitting of peaks in the Fourier transformed density of states, and second through the occurence of strong anomalous peaks. The anomalous peaks are very sharp, and disperse in a manner which is very similar to the conventional "octet" of peaks predicted in single-layer materials, but persist to energies which are higher than the coherence peak energy.

Acknowledgments

We acknowledge support of an undergraduate USRA by Trent University and NSERC of Canada. This work was also supported by Research Corporation grant CC6062, and by a Discovery Grant from NSERC of Canada.

[1] W. E. Pickett, Rev. Mod. Phys. 61, 433 (1989).

[2] S. Massida, J. Yu, and A. J. Freeman, Physica C 152, 251 (1988); H. Krakauer and W. E. Pickett, Phys. Rev. Lett. 60, 1665 (1988); M. S. Hybertsen and L. F. Mattheiss, ibid. 60, 1661 (1988).

[3] Andrea Damascelli, Zahid Hussain, Zhi-Xun Shen, Rev. Mod. Phys. 75, 473 (2003).

[4] Sudip Chakravarty, Asle Sudbø, Philip W. Anderson, and Steven Strong, Science 261, 337 (1993).

[5] D. L. Feng, N. P. Armitage, D. H. Lu, A. Damascelli, J. P. Hu, P. Bogdanov, A. Lanzara, F. Ronning, K. M. Shen, H. Eisaki, C. Kim, Z.-X. Shen, J.-I. Shimoyama, K. Kishio, Phys. Rev. Lett. 86, 5550 (2001); D. L. Feng, C. Kim, H. Eisaki,, D. H. Lu, A. Damascelli, K. M. Shen, F. Ronning, N. P. Armitage, N. Kaneko, M. Greven, J.-I. Shimoyama, K. Kishio, R. Yoshizaki, G. D. Gu, and Z.-X. Shen, Phys. Rev. B 65, 220501 (2002).

[6] A. A. Kordyuk, S. V. Borisenko, M. S. Golden, S. Legner, K. A. Nenkov, M. Knupfer, J. Fink, H. Berger, L. Forro, and R. Follath, Phys. Rev. B 66, 014502 (2002).

[7] Y. D. Chuang, A. D. Gromko, A. Fedorov, Y. Aiura, K. Oka, Yoichi Ando, H. Eisaki, S. I. Uchida, and D. S. Dessau, Phys. Rev. Lett. 87, 117002 (2001).

[8] S. V. Borisenko, A. A. Kordyuk, T. K. Kim, S. Legner, K. A. Nenkov, M. Knupfer, M. S. Golden, J. Fink, H. Berger, and R. Follath, Phys. Rev. B 66, 140509 (2002).

[9] M. C. Asensio, J. Avila, L. Roca, A. Tejeda, G. D. Gu, M. Lindroos, R. S. Markiewicz, and A. Bansil, Phys. Rev. B

67, 014519 (2003).
[10] Y.-D. Chuang, A. D. Gromko, A. V. Fedorov, Y. Aiura, K. Oka, Yoichi Ando, M. Lindroos, R. S. Markiewicz, A. Bansil, and D. S. Dessau, Phys. Rev. B 69 094515 (2004).
[11] P. T. Sprunger, L. Petersen, E. W. Plummer, E. Laegsgaard, and F. Besenbacher, Science 275, 1764 (1997).
[12] J. E. Hoffman, K. McElroy, D.-H. Lee, K. M. Lang, H. Eisaki, S. Uchida, and J. C. Davis, Science 297, 1148 (2002).
[13] K. McElroy, R. W. Simmonds, J. E. Hoffman, D.-H. Lee, J. Orenstein, H. Eisaki, S. Uchida, and J. C. Davis, Nature 422, 592 (2003).
[14] K. McElroy, D.-H. Lee, J. E. Hoffman, K. M. Lang, E. W. Hudson, H. Eisaki, S. Uchida, J. Lee, and J. C. Davis, cond-mat/0404005.
[15] C. Howald, H. Eisaki, N. Kaneko, M. Greven, A. Kapitulnik, Phys. Rev. B 67, 014533 (2003).
[16] Michael Vershinin, Shashank Misra, S. Ono, Y. Abe, Yoichi Ando, and Ali Yazdani, Science 303, 5666 (2004).
[17] Qiang-Hua Wang and Dung-Hai Lee, Phys. Rev. B 67, 020511 (2003).
[18] Lingyin Zhu, W. A. Atkinson, and P. J. Hirschfeld, Phys. Rev. B 69, 060503 (2004).
[19] Degang Zhang and C. S. Ting, Phys. Rev. B 67, 100506 (2003)
[20] L. Capriotti, D. J. Scalapino, and R. D. Sedgewick, Phys. Rev. B 68, 014508 (2003).
[21] T. Pereg-Barnea and M. Franz, Phys. Rev. B 68, 180506 (2003)
[22] C.-T. Chen and N.-C. Yeh, Phys. Rev. B 68, 220505 (2003).
[23] O. K. Andersen, A. I. Liechtenstein, O. Jepsen, and F. Paulsen, J. Phys. Chem. Solids, 56, 1573 (1995).
[24] A. A. Kordyuk, S. V. Borisenko, M. Knupfer, and J. Fink, Phys. Rev. B 67, 064504 (2003).
[25] S. V. Borisenko, A. A. Kordyuk, S. Legner, T. K. Kim, M. Knupfer, C. M. Schneider, J. Fink, M. S. Golden, M. Sing, R. Claessen, A. Yaresko, H. Berger, C. Grazioli, and S. Turchini, Phys. Rev. B 69, 224509 (2004).
[26] L. Dell'Anna, J. Lorenzana, M. Capone, C. Castellani, and M. Grilli, cond-mat/0407028.